

Article

# Blood Coagulation Activities of Cotton–Alginate–Copper Composites

Zdzisława Mrozińska<sup>1</sup>, Michał Ponczek<sup>2</sup> , Anna Kaczmarek<sup>1</sup> , Maciej Boguń<sup>1</sup>, Edyta Sulak<sup>1</sup> and Marcin H. Kudzin<sup>1,\*</sup>

<sup>1</sup> Łukasiewicz Research Network—Lodz Institute of Technology, 19/27 Marii Skłodowskiej-Curie Str., 90-570 Lodz, Poland

<sup>2</sup> Department of General Biochemistry, Faculty of Biology and Environmental Protection, University of Lodz, 90-236 Lodz, Poland

\* Correspondence: marcin.kudzin@lit.lukasiewicz.gov.pl; Tel.: +48-42-6163121

**Abstract:** Alginate-based materials have gained significant attention in the medical industry due to their biochemical properties. In this article, we aimed to synthesize Cotton–Alginate–Copper Composite Materials (COT-Alg<sup>(-)</sup>Cu<sup>(2+)</sup>). The main purpose of this study was to assess the biochemical properties of new composites in the area of blood plasma coagulation processes, including activated partial thromboplastin time (aPTT), prothrombin time (PT), and thrombin time (TT). This study also involved in vitro antimicrobial activity evaluation of materials against representative colonies of Gram-positive and Gram-negative bacteria and antifungal susceptibility tests. The materials were prepared by immersing cotton fibers in an aqueous solution of sodium alginate, followed by ionic cross-linking of alginate chains within the fibers with Cu(II) ions to yield antimicrobial activity. The results showed that the obtained cotton–alginate–copper composites were promising materials to be used in biomedical applications, e.g., wound dressing.

**Keywords:** alginic acid; antifungal activity; antimicrobial activity; blood coagulation; composite; copper; cotton-based materials; composite; activated partial thromboplastin time; polymer functionalization; prothrombin time; thrombin time



**Citation:** Mrozińska, Z.; Ponczek, M.; Kaczmarek, A.; Boguń, M.; Sulak, E.; Kudzin, M.H. Blood Coagulation Activities of Cotton–Alginate–Copper Composites. *Mar. Drugs* **2023**, *21*, 625. <https://doi.org/10.3390/md21120625>

Academic Editors: Maila Castellano and Andrea Dodero

Received: 16 October 2023

Revised: 23 November 2023

Accepted: 27 November 2023

Published: 30 November 2023



**Copyright:** © 2023 by the authors. Licensee MDPI, Basel, Switzerland. This article is an open access article distributed under the terms and conditions of the Creative Commons Attribution (CC BY) license (<https://creativecommons.org/licenses/by/4.0/>).

## 1. Introduction

Cotton is a natural fiber composed mainly of pure cellulose, and it is commonly applied in the apparel and textile industry [1,2]. This is due to its favorable properties, including softness, mechanical strength, elasticity, and water affinity [1]. Moreover, it is a low-cost and biodegradable material [1]. Apart from that, cotton exhibits a set of properties that are very desirable for medical and biomedical applications, including a porous structure, a large surface area, and gas permeability [2]. Thus, it is widely employed for the production of health care textiles [2]. The use of cotton for medical purposes may be divided into two categories: external and internal biomaterials [2]. The first group includes medical clothing (such as gowns, masks, uniforms, and caps), surgical covers and drapes, as well as beddings [2]. The second one constitutes products used for tissue engineering, dental and surgical applications, drug delivery systems, as well as wound dressings [2].

As far as wound dressings are concerned, cotton gauze is one of the most popular and widely used wound dressings [2]. It is a dry wound dressing with a fibrous structure, and it has the ability to absorb the wound exudate [2]. However, it saturates very quickly and requires frequent changing, which is not cost effective [2]. Another drawback of a cotton gauze is its adherence to the wound, which causes damage to the tissue during its removal [2]. Moreover, cotton does not exhibit antimicrobial activity; thus, it is prone to microbial contamination, leading to the development of infection [1,2]. Therefore, cotton gauze is mainly applied as a secondary dressing or for wounds with low exudate, while its use for chronic, highly exuding wounds, such as burns or ulcers, is highly limited [2].

Therefore, researchers are currently focused on the development of more advanced wound dressings based on multifunctional textiles [1,2]. These attempts involve the surface modification of cotton (for example, using different biopolymers, such as chitosan or alginate), in order to overcome the abovementioned disadvantages of traditional cotton gauze wound dressings [1–4].

Alginate is a polysaccharide of natural origin usually derived from brown seaweed but also from bacteria [5–18]. It is a hydrophilic, water-soluble anionic biopolymer containing blocks of (1,4)-linked- $\beta$ -D-mannuronate (M) and  $\alpha$ -L-guluronate (G) residues [5,7–19] (Figure 1).

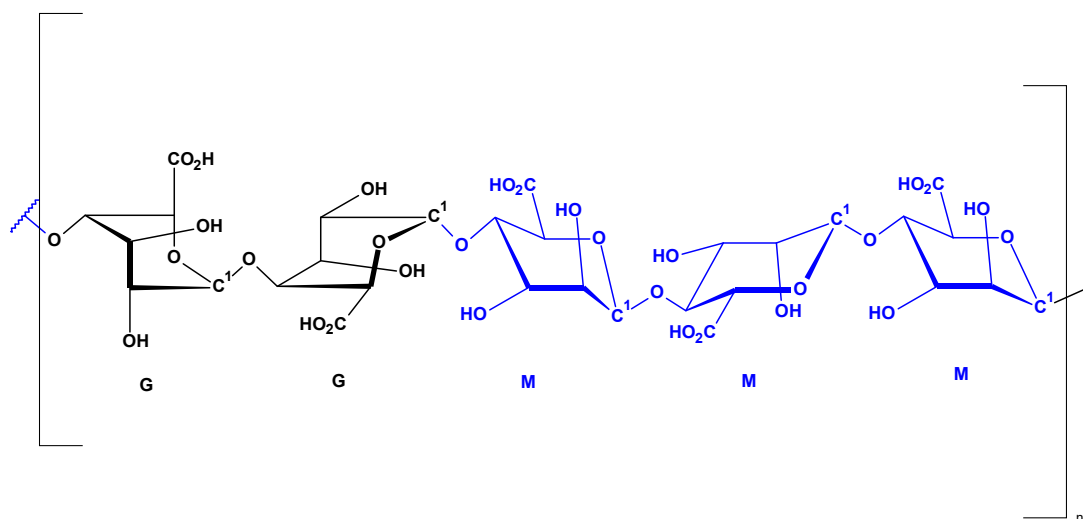


**Figure 1.** Structure of GGMMM fragment of alginic acid (M— $\beta$ -D-Mannuronate and G— $\alpha$ -L-guluronate).

Alginate is well known from its remarkable properties, such as chemical versatility, biocompatibility, biodegradability, non-immunogenicity, non-toxicity, and biological activity [5,7–18,20,21]. Moreover, it is the second most abundant biopolymer available (after cellulose), and its extraction and processing costs are relatively low [7]. Finally, alginate has a very good cross-linking capability, and it is easy to process and modify [8,14,17,21]. This is due to its distinct physical and chemical structure, including, mainly, the presence of free hydroxyl and carboxyl groups, as well as its sol-to-gel transformation ability [5,8]. This not only allows it to develop alginate-based composites with specific chemical and physical properties but also makes alginate a perfect material used to finish textiles (for instance, cotton) [8]. Currently, there are multiple different techniques used for textile functionalization using alginate, such as nanocomposite coating, ionic cross-linking coating, and layer-by-layer coating [8].

Due to the abovementioned outstanding properties, alginate is gaining a lot of interest in terms of its biological and medical applications, mainly for tissue engineering and wound healing [5–23]. It is believed that alginate-based wound dressings provide an appropriate drainage of wound exudates and prevent the entry of pathogenic bacteria [9–13]. Alginate’s high content of water allows it to ensure the proper moist environment [5], which in turn helps to keep the optimal pH [18,24]. This is of the utmost importance because it was proven that a wet environment is considerably more effective in terms of wound healing [2]. Furthermore, alginate exhibits a unique hemostatic effect owing to its gel-forming ability and high adsorption capacity [19]. According to the literature, the water absorption rate of an alginate fiber is equal to 2.2 times its mass [15]. Alginate-based dressings absorb blood and body fluids and form hydrogels, which adhere to the surface of the wound, leading to the compression of the bleeding wound [15,25]. Additionally, due to the presence of mannuronic (M) or guluronic (G) groups with high calcium (Ca) content, alginates serve as donors of calcium ions [26], which enter the wound as a result of the ion exchange reaction

with sodium ions present in blood [15,20]. Calcium ions are responsible for the stimulation of clotting factors (VII, IX, X), activation of the coagulation cascade reaction, and platelet aggregation [15,22]. It was also reported, that depending on its structure and M or G group composition, alginate may influence blood coagulation to different extents [22]. Moreover, some studies suggest that alginate promotes the growth of the new epidermis [5]. Thus, alginate-based materials are considered to accelerate the process of hemostasis and wound healing [15,18,21,23,24].

Another additional factor that has to be taken into account when it comes to effective wound dressing materials is the inhibition of bacterial growth. According to some studies, the alginate-based materials exhibit antimicrobial activity [3,18,27]. For instance, Rafiq et al. pointed out that alginate interacts with a bacterial outer surface through negative charges and, as a consequence, causes the disruption of bacteria [5,28]. What is more, alginates were demonstrated to kill microorganisms as they block the nutrient transportation by forming a viscous layer around them [5]. Nevertheless, the observed antimicrobial effect is insufficient in terms of wound healing. Thus, alginate composite materials composed of various additives are investigated with the aim of enhancing different properties, including not only antibacterial activity, but also cell viability and adhesion, as well as blood clotting within hemostasis. Among the different antimicrobial agents, copper is attracting growing attention.

On the one hand, copper in its ionized form as a trace element is a transition metal necessary for the proper functioning of the human organism, being a cofactor of many copper enzymes participating in redox reactions, and, on the other hand, the biocidal properties of copper and its complexes have been well documented in the literature [29–37]. Furthermore, despite the high susceptibility of microorganisms to copper, human tissues do not exhibit sensitivity towards it, as it is needed for their proper functioning [38–40]. Additionally, copper is also significantly cheaper than silver, which is a very popular antimicrobial agent [32,41]. Therefore, copper is considered to be a very effective additive used for the antimicrobial functionalization of alginate-based materials as well as textiles [42–48]. Moreover, copper plays an important role in the wound-healing process [47–51]. This is due to the stimulation of the activity of copper-dependent enzymes, proteins, and polysaccharides, which results in the positive influence on the matrix remodelling, cell proliferation, and reepithelization [49–51]. Furthermore, copper takes part in the generation of the vascular endothelial growth factor and thus affects the angiogenesis [49,50,52,53]. In addition, copper is responsible for the stabilization of fibrinogen and collagen, and it increases the expression of integrin [40,50,54].

The main biological aim of the current study is to test if the new cotton–alginate–copper-based materials with optimally selected metallic component concentration have any detrimental effect on blood plasma coagulation as the first step during wound care, while maintaining antimicrobial effects. Therefore, aPTT and PT measurements have been carried out. aPTT enables the study of the intrinsic (contact) blood plasma coagulation pathway and reveals the time of fibrin clot formation after activation on a negatively charged surface (in the presence of kaolin) where contact factors (XII, XI), plasma prekallikrein (PK), and high molecular kininogen (HK) initiate the blood coagulation cascade. PT is used to study blood clotting triggered by extrinsic pathway (tissue factor—thromboplastin, calcium ions), where tissue factor (TF) activates factor VII, thus leading to fibrin formation, when a prothrombinase complex is formed [55]. In this way, both pathways of the plasma component of blood coagulation can be tested using aPTT and PT.

## 2. Results and Discussion

### 2.1. Preparation of Composite Material

The cotton fabric samples were modified through a dip-coating, two-step method, based on our previous work related to the modification of poly(lactic acid) fiber materials [40,56]. Samples of cotton fabric (COT) were impregnated in a homogeneously dispersed polysaccharide solution for 1 min (0.5%—COT-ALG<sup>(-)</sup>Na<sup>(+)</sup>-1 and 5%—COT-

ALG<sup>(-)</sup>Na<sup>(+)</sup>-2) and then immediately transferred into two different aqueous solutions of copper (II) chloride and re-immersed for 1 min (COT-ALG<sup>(-)</sup>Cu<sup>(2+)</sup>-1—5% CuCl<sub>2</sub> solution, COT-ALG<sup>(-)</sup>Cu<sup>(2+)</sup>-2 in 10% CuCl<sub>2</sub>) (Figure 2). Then, the alginate composites were squeezed and dried for 6 h at 40 °C to constant weight. For the biological and biochemical comparative research, we modified cotton fabric samples using analogous concentrations of copper solution without alginate modification.

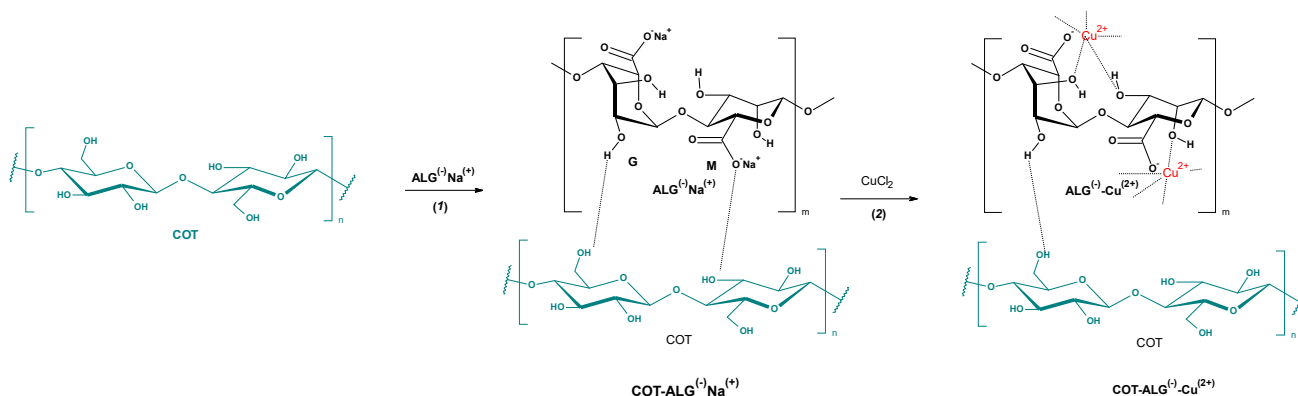


**Figure 2.** The schematic diagram of the procedures for surface modification of cotton material using alginate.

Table 1 presents abbreviations of the cotton samples used for the investigation. Because the parts of these abbreviations contain chemical formulas, we used COT for cotton instead of CO/Co (CO and/or Co can be confused with carbon oxide or cobalt).

**Table 1.** Composition of the alginate dip-coating solution (%).

Sample Assignments/Name	Mixture Components of Film-Forming Material (%)			
	Sodium Alginate Solution		Copper(II) Chloride Solutions	
	0.5%	5%	5%	10%
COT	—	—	—	—
COT-ALG <sup>(-)</sup> Na <sup>(+)</sup> -1 (a)	+	—	—	—
COT-ALG <sup>(-)</sup> Na <sup>(+)</sup> -2 (a)	—	+	—	—
COT-ALG <sup>(-)</sup> Cu <sup>(2+)</sup> -1	+	—	+	—
COT-ALG <sup>(-)</sup> Cu <sup>(2+)</sup> -2	+	—	—	+
COT-Cu <sup>(2+)</sup> -1	—	—	+	—
COT-Cu <sup>(2+)</sup> -2	—	—	—	+

(a) Gravimetric analysis of COT-ALG<sup>(-)</sup>Na<sup>(+)</sup> samples led to estimation that COT-ALG<sup>(-)</sup>Na<sup>(+)</sup>-1 contained 1% alginate and COT-ALG<sup>(-)</sup>Na<sup>(+)</sup>-2 contained 9.7% alginate. These composites were coded in the text as COT-ALG<sup>(-)</sup>Na<sup>(+)</sup>(1%) and COT-ALG<sup>(-)</sup>Na<sup>(+)</sup>(9.7%), respectively.

## 2.2. Chemical and Structural Characterization

### 2.2.1. Fourier Transform Infrared Spectroscopy

Characteristic FTIR bands  $\nu$  (cm<sup>-1</sup>) determined for COT fabrics, alginate salts, and copper composites (ALG<sup>(-)</sup>Na<sup>(+)</sup>, ALG<sup>(-)</sup>Cu<sup>(2+)</sup> and COT-ALG<sup>(-)</sup>Cu<sup>(2+)</sup>) are presented in Figure 3. Table 2 lists infrared spectroscopy absorptions by frequency regions in the spectral range of 4000–400 cm<sup>-1</sup> of the samples, with the designation of chemical bonds. The comparison between the FTIR spectra of the alginic acid sodium salt and cotton fabric indicates the presence of main absorption bands in the cotton–alginate–copper composite (COT-ALG<sup>(-)</sup>Cu<sup>(2+)</sup>), which is confirmed by the data from the literature [57–65].

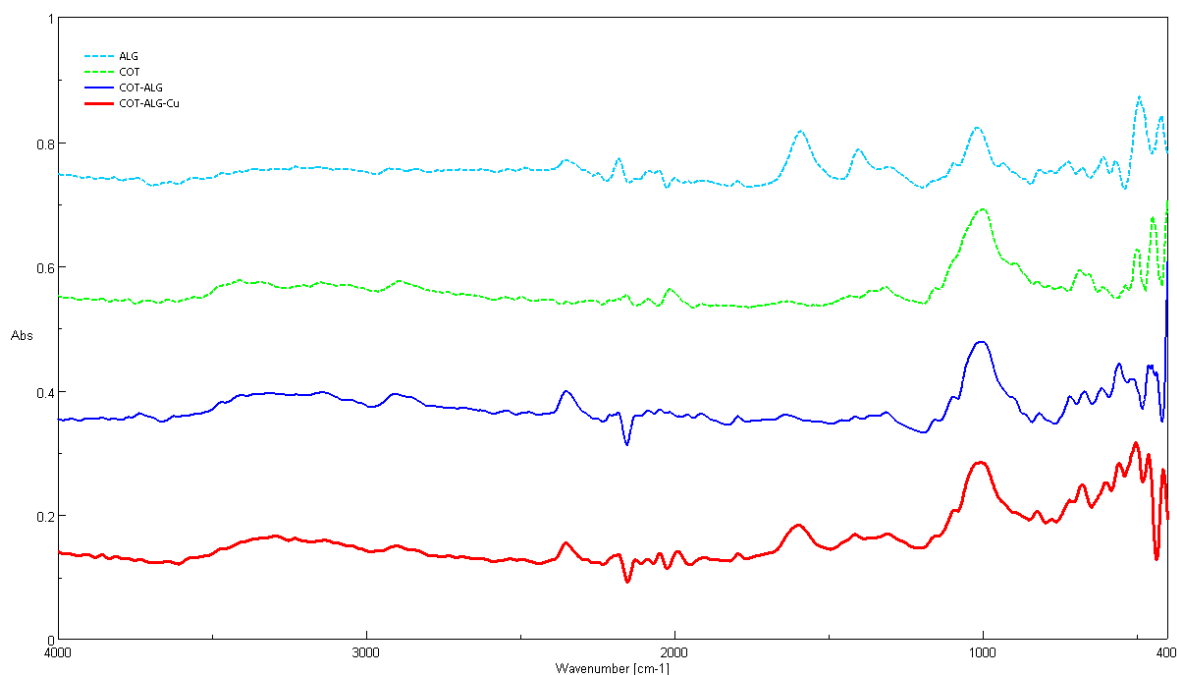


**Figure 3.** Fourier transform infrared spectroscopy (FTIR) spectra of: alginic acid sodium salt (ALG); cotton fabric (COT); cotton–alginate composite (COT-ALG<sup>(−)</sup>Na<sup>(+)</sup>(1%)); cotton–alginate–copper composite (COT-ALG<sup>(−)</sup>Cu<sup>(2+)</sup>(0.15)).

**Table 2.** Characteristic FTIR bands  $\nu$  (cm<sup>−1</sup>) determined for COT nonwoven, alginate salts ALG<sup>(−)</sup>Na<sup>(+)</sup>, and COT-ALG<sup>(−)</sup>Cu<sup>(2+)</sup>(0.15) composite.

Lit: Cellulose		Lit: ALG <sup>(−)</sup> Na <sup>(+)</sup>		Sample: COT		Sample: COT-ALG <sup>(−)</sup> Cu <sup>(2+)</sup>	
( $\nu$ /cm <sup>−1</sup> )	Assign./ (Ref.) [57]	Lit. Bands $\nu$ (cm <sup>−1</sup> ) [58–62]	Assign./ (Ref.) [58]	$\nu$ (cm <sup>−1</sup> )	Int./ <sup>(a)</sup>	$\nu$ (cm <sup>−1</sup> )	Int./ <sup>(a)</sup>
3300	$\nu_s$ O-H	3350 ± 350	$\nu_s$ O-H	3400	0.04/ <sup>(b)</sup>	3292	0.11
2893	$\nu_s$ C-H	2926 ± 1	$\nu_s$ C-H	2887	0.05	2900	0.09
		1650	$\nu_{as}$ COO <sup>−</sup>				
		1614	$\nu_{as}$ COO <sup>−</sup>			1590	0.13
1429	$\gamma$ O-H	1417	$\delta$ C-H, $\nu_s$ COO <sup>−</sup>	1428	0.02	1417	0.12
1370	$\gamma$ CH <sub>2</sub>			1308	0.03	1305	0.12
1120	$\nu_{as}$ C-O-C	1301 (ms)	$\delta$ C-H	1150	0.03	1150	0.1
		1096 (s)	$\nu$ C-O, $\nu$ C-C, $\delta$ C-C-O			1094	0.15
1060	$\nu_s$ C-C-O	1124 (s)	$\nu$ C-O, $\nu$ C-C, $\delta$ C-C-C, $\nu_{as}$ C-O-C/ <sup>(c)</sup>				
1000	$\nu$ C-C	1034 (vs)	$\nu_{as}$ C-O-C/ <sup>(c)</sup> , $\nu$ C-O/ <sup>(c)</sup> , $\nu$ C-C	1000	0.15	1007	0.23
893	$\nu$ C <sup>1</sup>			892	0.07		

Table 2. Cont.

Lit: Cellulose		Lit: ALG <sup>(-)</sup> Na <sup>(+)</sup>		Sample: COT		Sample: COT-ALG <sup>(-)</sup> Cu <sup>(2+)</sup>	
( $\nu/\text{cm}^{-1}$ )	Assign./ (Ref.) [57]	Lit. Bands $\nu$ ( $\text{cm}^{-1}$ ) [58–62]	Assign./ (Ref.) [58]	$\nu$ ( $\text{cm}^{-1}$ )	Int./ <sup>(a)</sup>	$\nu$ ( $\text{cm}^{-1}$ )	Int./ <sup>(a)</sup>
		776 (w)	rb, $\delta$ C–C–H, $\delta$ C–C–O				
		703(ms)	rb $\delta\omega$ O–H				
670	$\omega$ O–H	826 (ms)	$\delta$ C–O–C/ <sup>(c)</sup> , $\delta$ C–C–C, $\delta$ C–C–O/ <sup>(c)</sup> , $\delta$ C–C–H, $\delta\omega$ O–H	684	0.06	673	0.19

<sup>(a)</sup> Band assignment:  $\nu$ —stretching vibration;  $\delta$ —deformation; sh—shoulder; s—symmetric; as—asymmetric; r—rocking;  $\gamma$ —bending mode;  $\omega$ —wagging; rb—ring breathing. <sup>(b)</sup> Band intensity: the bands with absorbance values  $\geq 0.005$  were listed and subsequently approximated to a second decimal place. For data from the literature: s—strong, vs—very strong, ms—medium strong, w—weak. <sup>(c)</sup> Glycosidic linkage.

### 2.2.2. Flame Atomic Absorption Spectrometry

Determination of the Cu concentration in the cotton–alginate–copper composite samples was performed by means of FAAS spectrometry, and the results are shown in Table 3.

Table 3. Copper concentration in alginate composite samples.

Sample	Cu Concentration			Ultimate Forms of Samples Abbreviations
	(g/kg)	% (g/100 g)	MI (mol/kg)	
COT	0.002	0.0002	0.00003	
COT-ALG <sup>(-)</sup> Na <sup>(+)</sup> -1	0.002	0.0002	0.00003	COT-ALG <sup>(-)</sup> Na <sup>(+)</sup> (1%)
COT-ALG <sup>(-)</sup> Na <sup>(+)</sup> -2	0.002	0.0002	0.00003	COT-ALG <sup>(-)</sup> Na <sup>(+)</sup> (9.7%)
COT-Cu <sup>(2+)</sup> -1	10.06	1.01	0.16	COT-Cu <sup>(2+)</sup> (0.16)
COT-Cu <sup>(2+)</sup> -2	19.19	1.92	0.30	COT-Cu <sup>(2+)</sup> (0.30)
COT-ALG <sup>(-)</sup> Cu <sup>(2+)</sup> -(1)	9.35	0.935	0.147	COT-ALG <sup>(-)</sup> Cu <sup>(2+)</sup> (0.15)
COT-ALG <sup>(-)</sup> Cu <sup>(2+)</sup> -(2)	17.51	1.75	0.276	COT-Alg <sup>(-)</sup> Cu <sup>(2+)</sup> (0.28)

COT-ALG<sup>(-)</sup>Na<sup>(+)</sup>(%) samples—% percentage concentration of alginate in corresponding COT-ALG<sup>(-)</sup>Na<sup>(+)</sup> composites (1% or 9.7%); COT-ALG<sup>(-)</sup>Cu<sup>(2+)</sup>(MI) samples—MI molal concentration of copper in corresponding COT-ALG<sup>(-)</sup>Cu<sup>(2+)</sup>(MI) composites (0.15 molal or 0.28 molal). The results have been measured in triplicate and are presented as a mean value with  $\pm$  deviation equal to approximately 2%.

The results of the determination of the copper concentration in the composites show that the metal content in complex materials depends on the variant of the applied modifier dip-coating solution and the type of solution of CuCl<sub>2</sub> (Table 1). The higher concentration of the used copper (II) chloride solutions (10%) resulted in the higher content of the metal in the cotton–alginate composite (17.51 g/kg) and cotton sample (COT-Cu<sup>(2+)</sup>(0.30)—19.19 g/kg), and the lower concentration of the Cu solution (5%) gave a relatively lower content of Cu in the sample (COT-Alg<sup>(-)</sup>Cu<sup>(2+)</sup>(0.15)—9.35 g/kg/COT-Cu<sup>(2+)</sup>(0.16)—10.06 g/kg). Additionally, the FAAS spectrometry measurements also indicated that the distribution of copper in the material is quite uniform (approximately 4.5%).

### 2.2.3. Morphology and Elemental Analysis

#### Microscopy Analysis

The analysis of changes in the morphological and elemental structure of the surface and fibers of cotton fabric after modification was carried out using a digital microscope with the laser-based elemental analyzer. Figure 4 shows microscope images of the samples before and after modification processes under the magnifications equal to  $\times 500$  and  $\times 2500$ . Table 4 shows the quantitative analysis of the content of elements on the fiber surface based on the laser-based elemental analyzer.

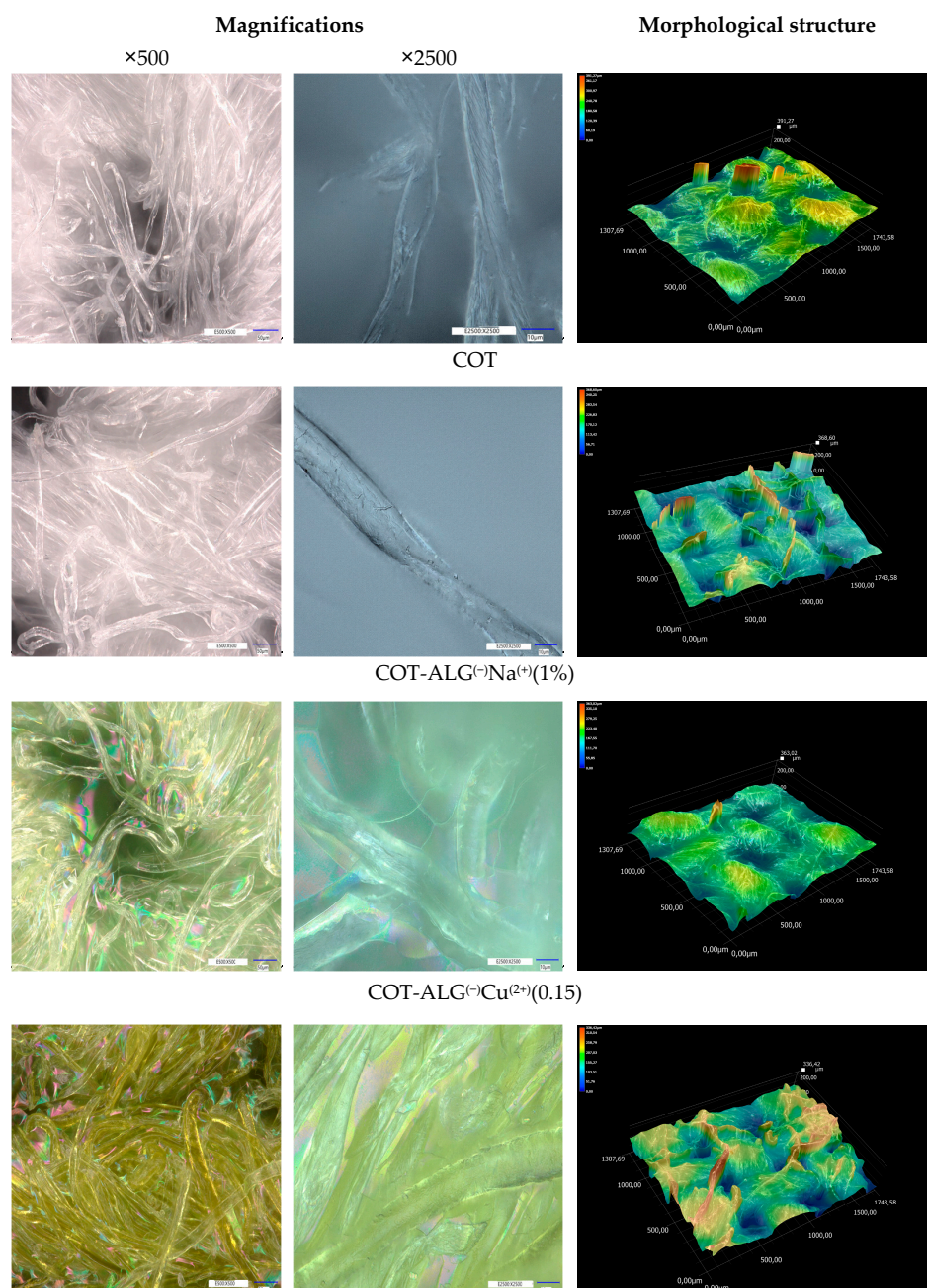


**Figure 4.** Optical microscopy images (magnifications:  $\times 500$ ,  $\times 2500$ ) and morphological visualization of surface structure of samples before and after modification processes.

**Table 4.** Elemental compositions of the composites investigated based on the laser-based elemental analyzer (SCLA).

Sample	Analysis	Quantitative Content of Elements of Samples (wt.%)			
		C	H	O	Cu
COT	SCLA	35	9	56	-
	BCEA	44.4	6.22		
	CEC <sup>(a)</sup>	(44.4)	(6.17)	(49.4)	
ALG <sup>(-)</sup> Na <sup>(+)</sup> × 2H <sub>2</sub> O	CEC <sup>(a)</sup>	(30.8)	(4.70)	(54.7)	
ALG <sup>(-)</sup> Na <sup>(+)</sup> × nH <sub>2</sub> O [66]	BCEA	29.	4.5		
COT-ALG <sup>(-)</sup> Cu <sup>(2+)</sup> (0.15) <sup>(c)</sup>	SCLA	33	9	54	4
	BCEA				0.94 <sup>(b)</sup>
COT-ALG <sup>(-)</sup> Cu <sup>(2+)</sup> (0.28) <sup>(c)</sup>	SCLA	28	9	50	13
	BCEA				1.75 <sup>(b)</sup>

Methods: BCEA—Bulk Composition Elemental Analysis based on Combustion Elemental Analysis; CEC—Calculated Elemental Composition (data in brackets); SCLA—Surface Composition Laser Analysis (the results have been measured in duplicate and are presented as a mean value with  $\pm$  deviation equal to approximately 2%); <sup>(a)</sup> CEC data for cellulose (C<sub>6</sub>H<sub>10</sub>O<sub>5</sub>)<sub>n</sub> ( $n \times 162$ ) and/or sodium alginate (C<sub>6</sub>H<sub>7</sub>O<sub>6</sub>Na × 2H<sub>2</sub>O)<sub>n</sub> ( $n \times 234$ ), respectively; <sup>(b)</sup> Data taken from Table 3; <sup>(c)</sup> COT-ALG<sup>(-)</sup>Cu<sup>(2+)</sup>(M) samples—Ml—molal concentration of copper in corresponding COT-ALG<sup>(-)</sup>Cu<sup>(2+)</sup> composites (0.15 molal or 0.28 molal).

As far as the morphology of the investigated samples is concerned, it may be observed that the modification of the samples with alginate (COT-Alg<sup>(-)</sup>Na<sup>(+)</sup>) and copper (II) chloride (COT-Alg<sup>(-)</sup>Cu<sup>(2+)</sup>) caused some noticeable changes. The two-step dip-coating modification led to the formation of the film interconnecting the cotton fibers, which is especially apparent for the COT-Alg<sup>(-)</sup>Cu<sup>(2+)</sup>(0.28) sample. At the same time, the pores become less visible, which may be due to the fact that the void spaces were filled with the alginate and copper. This was also confirmed by the 3D microscopic images showing the morphological structure of the samples, which revealed that the modification of the cotton resulted in the smoother surfaces, i.e., the height difference between the lowest and the highest points on the surface decreased. Similar results were observed in our previous study for the PLA nonwovens modified with sodium alginate and zinc (II) chloride [56].

The observations under the higher magnification ( $\times 2500$ ) revealed that the modification of the cotton samples with alginate and CuCl<sub>2</sub> did not cause any significant damage to the fibers.

The laser-based elemental analysis (Table 4) of the surface of the investigated samples confirmed the presence of the elements, which were the structural components of both cellulose and alginate, i.e., oxygen, carbon, and hydrogen. In the case of the samples modified with copper (II) chloride, the copper was also present on the surface, and its concentration increased with the increasing concentration of the CuCl<sub>2</sub> in the solution used for the modification.

As far as the quantitative analysis is concerned, it was observed that in the case of the sample modified with sodium alginate only, the concentration of hydrogen increased, while the concentration of carbon decreased. In the case of samples modified with copper (II) chloride, the relative content of carbon and oxygen slightly decreased due to the appearance of copper on the surface. The concentration of copper increased from 4 to 13 wt. % with the increase in the CuCl<sub>2</sub> concentration in the solution from 5 to 10%. The increase in the copper concentration is in agreement with the results obtained through FAAS, which also revealed the increase in the copper content for the sample COT-ALG<sup>(-)</sup>Cu<sup>(2+)</sup>(0.28). The analysis of the data also revealed substantial differences in the bulk and surface elemental content. Thus, for cotton, the carbon concentration was over 20% lower for the surface than in bulk, whereas hydrogen is over 30% higher. These data suggest that surface carbon atoms

were covered by hydrogens. Surface carbon contents in COT-ALG<sup>(-)</sup>Cu<sup>(2+)</sup> composites were lower than for unmodified cotton due to lower carbon contents in ALG<sup>(-)</sup>Na<sup>(+)</sup> in comparison with COT. Lowering of the surface contents of carbon and oxygen during the increase in the copper charge in COT-ALG<sup>(-)</sup>Cu<sup>(2+)</sup> resulted from the increase in the copper content as well as the masking effect of the smaller atoms, i.e., C and H, by large copper atoms. It is worth noting that the surface content of copper atoms is 4–7.5 times higher than in bulk.

#### Specific Surface Area

The total pore volume and specific surface area of the cotton sample (COT) and copper-alginate composites (COT-ALG<sup>(-)</sup>Na<sup>(+)</sup>, COT-ALG<sup>(-)</sup>Cu<sup>(2+)</sup>) are presented in Table 5.

**Table 5.** The specific surface area and total pore volume for the unmodified cotton sample (COT) and cotton–alginate composites (COT-ALG<sup>(-)</sup>Na<sup>(+)</sup> and COT-ALG<sup>(-)</sup>Cu<sup>(2+)</sup>).

Sample Name	Specific Surface Area (m <sup>2</sup> /g)	Total Pore Volume (cm <sup>3</sup> /g)
COT	0.7359	$7.408 \times 10^{-3}$
COT-ALG <sup>(-)</sup> Na <sup>(+)</sup> (1%)	0.6191	$3.095 \times 10^{-3}$
COT-ALG <sup>(-)</sup> Na <sup>(+)</sup> (9.7%)	0.5577	$2.840 \times 10^{-3}$
COT-ALG <sup>(-)</sup> Cu <sup>(2+)</sup> (0.15)	0.6042	$3.033 \times 10^{-3}$
COT-ALG <sup>(-)</sup> Cu <sup>(2+)</sup> (0.28)	0.5931	$2.998 \times 10^{-3}$

The results have been measured in duplicate and are presented as a mean value with  $\pm$  deviation equal to approximately 2%.

The modification of cotton material with alginate (COT-ALG<sup>(-)</sup>Na<sup>(+)</sup>) and copper (II) chloride (COT-ALG<sup>(-)</sup>Cu<sup>(2+)</sup>) leads to the lowering of the specific surface area and total pore volume (BET). The specific surface area of the cotton material (COT) sample was equal to 0.7359 m<sup>2</sup>/g. The modification of cotton fabric in the solution of alginic acid sodium salt resulted in the decrease of the specific surface area to 0.6191 m<sup>2</sup>/g (COT-ALG<sup>(-)</sup>Na<sup>(+)</sup>(1%)). With the increase in the concentration of the sodium alginate, the specific surface area decreased even further to 0.5577 m<sup>2</sup>/g. Similarly, the subsequent immersion in a copper(II) chloride solution (COT-ALG<sup>(-)</sup>Cu<sup>(2+)</sup>(0.15)/(0.28)) also resulted in the lowering of the specific surface area; however, the observed changes were not significant. The higher the concentration of Cu, the lower the specific surface area (0.6042 and 0.5931 m<sup>2</sup>/g, respectively).

At the same time, a significant decrease in the total pore volume for the modified samples may be observed from  $7.408 \times 10^{-3}$  cm<sup>3</sup>/g to  $3.095 \times 10^{-3}$ – $2.840 \times 10^{-3}$  cm<sup>3</sup>/g. In the case of the cotton samples modified with the solution of alginic acid sodium salt, the higher the concentration of sodium alginate, the lower the total pore volume observed. Further modification with copper (II) chloride also caused a decrease in the total pore volume; however, the change was not as significant. A similar trend may be observed as was noted earlier, i.e., a higher concentration of Cu leads to a slightly lower total pore volume.

The observed decrease in the specific surface area and total pore volume is probably due to the fact that the pores present in the samples were filled with the sodium alginate and copper used for the modification. This is in agreement with the fact that increasing sodium alginate and copper concentration resulted in the lowering of the total pore volume and specific surface area. The decrease in the porosity caused the decrease of the specific surface area as a consequence. The obtained results are in agreement with the morphological analysis of the surface of the investigated samples, which revealed that the pores became less visible due to the performed modifications, and the observed surfaces became smoother as a result of the formation of the film interconnecting the cotton fibers.

In conclusion, the most significant change in the specific surface area and total pore volume was observed for the modification with a 0.5% solution of sodium alginate. A further increase in the sodium alginate concentration and the subsequent immersion in  $\text{CuCl}_2$  solution, as well as an increase in the concentration of Cu, resulted only in a slight change in the observed parameters.

Figure 5 presents the  $\text{N}_2$  adsorption–desorption isotherms obtained for the investigated samples. For all of the samples, the amount of adsorbate increases exponentially with the growing pressure. Because the obtained absorption isotherms resemble the hyperbolic graph with no distinct “knee” formed, they can be classified as type III according to the IUPAC classification [65,67]. The type III isotherm is characterized by its non-porous and/or macroporous materials, and it is typically observed for relatively weak interactions between the adsorbent and adsorbate [65,67]. This type of isotherm is associated with low uptake at a low concentration followed by the significant increase in sorption at higher vapor concentration [65,67]. The lack of a distinctive “knee” associated with the formation of a well-defined monolayer indicates that the sorption occurs fully according to the multilayer mechanism [65,67].

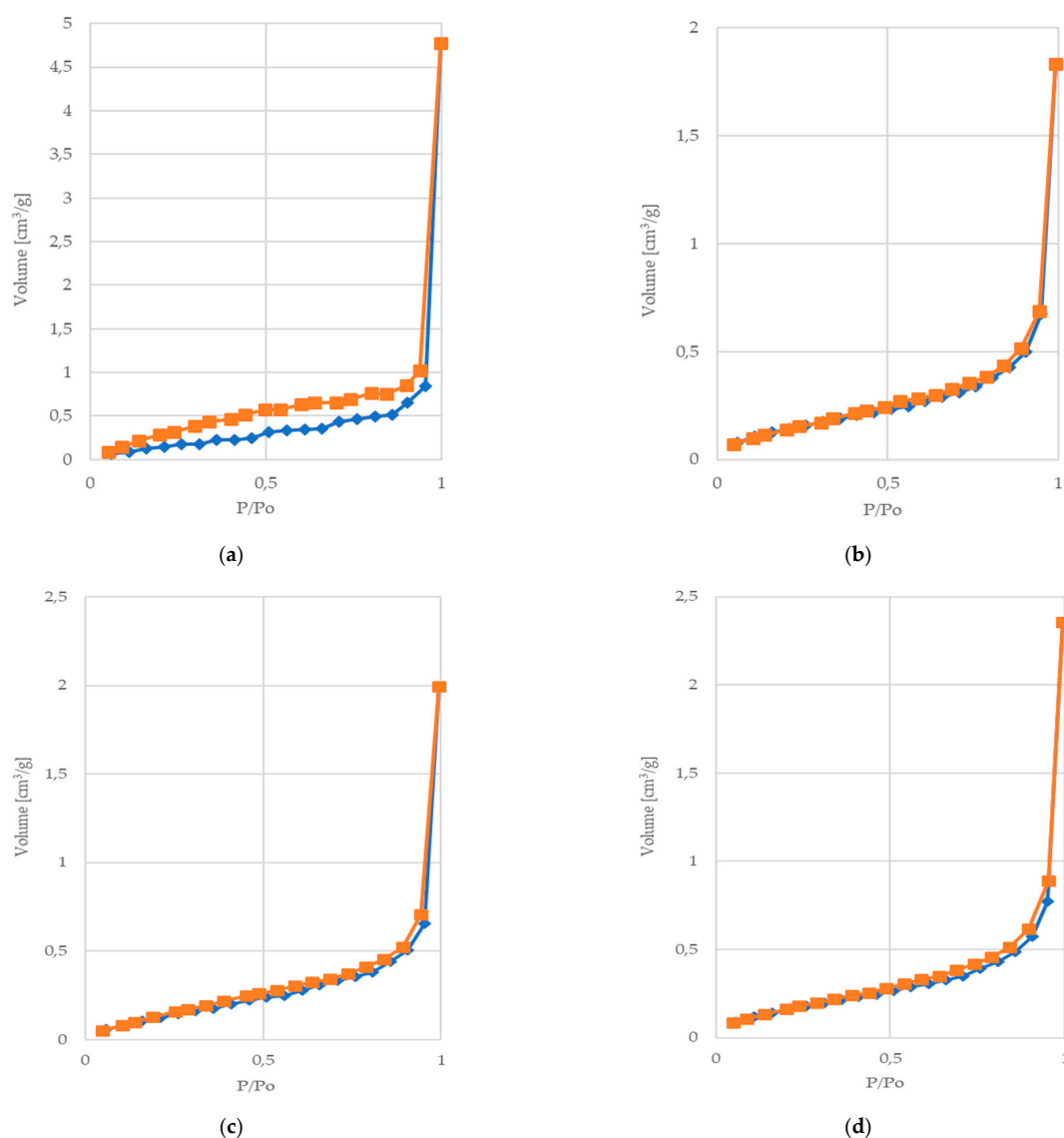


**Figure 5.** Isotherms of nitrogen adsorption/desorption at 77 K in the various types of materials studied in this work: (a) COT; (b) COT- $\text{ALG}^{(-)}\text{Na}^{(+)}$ (1%); (c) COT- $\text{ALG}^{(-)}\text{Cu}^{(2+)}$ (0.16); (d) COT- $\text{ALG}^{(-)}\text{Cu}^{(2+)}$ (0.28). Lines are results of approximation.

The presence of the hysteresis loop, i.e., the difference between the adsorption and desorption isotherms, is usually related to the capillary condensation in mesopore structures [65,67,68]. It occurs due to the fact that capillary condensation takes place at a higher relative pressure than capillary evaporation [65]. In the case of the obtained isotherms, the type H3 hysteresis loop may be observed for all of the samples. This type of hysteresis loop occurs when the macropores are not fully filled with pore condensate, and it is typical of slit-shaped pores [65,67,68]. The size of the observed loops decreases significantly for the modified samples, which may be associated with the observed lower total pore volume.

#### 2.2.4. Air Permeability

Determination of the air permeability of cotton–alginate–copper composites was carried out according to the EN ISO 9237:1998 standard [69], and all results are shown in Table 6.

**Table 6.** The air flow resistance of COT, COT-ALG<sup>(-)</sup>Na<sup>(+)</sup>, and COT-ALG<sup>(-)</sup>Cu<sup>(2+)</sup> sample according to the EN ISO 9237: 1998 standard [69].

Parameter	COT	COT-ALG <sup>(-)</sup> Na <sup>(+)</sup> (1%)	COT-ALG <sup>(-)</sup> Na <sup>(+)</sup> (9.7%)	COT-ALG <sup>(-)</sup> Cu <sup>(2+)</sup> (0.15)	COT-ALG <sup>(-)</sup> Cu <sup>(2+)</sup> (0.28)
Average air permeability (mm/s)	810 ± 7	278 ± 35	39.3 ± 3.8	283 ± 41	286 ± 35

The results have been measured in duplicate and are presented as the mean value with ± deviation of approximately 2%.

The results indicate that alginate modification decreased the air permeability of all coated samples. The higher concentration of alginate used during the modification (COT-ALG<sup>(-)</sup>Na<sup>(+)</sup>(9.7%)) reduced the permeability of the composite (from 278 to 39.3 mm/s). At the same time, the permeability was not significantly affected by the modification with copper chloride (COT-ALG<sup>(-)</sup>Cu<sup>(2+)</sup>: 283/286 mm/s). The samples modified with different concentration of CuCl<sub>2</sub> had approximately similar result of air permeability (COT-ALG<sup>(-)</sup>Cu<sup>(2+)</sup>(0.15)/(0.28): 283/286 mm/s). The decrease in air permeability for the modified samples may be associated with the lowering of the total pore volume due to the filling of pores with the sodium alginate and copper. The most significant change in the air permeability corresponds to the lowest value of the total pore volume.

#### 2.2.5. Tensile Testing

The results of the tensile strength measurements (durability for stretching and relative elongation at maximum load) of the cotton–alginate–copper composites are listed in Table 7.

**Table 7.** Tensile strength test of COT, COT-ALG<sup>(-)</sup>Na<sup>(+)</sup>, and COT-ALG<sup>(-)</sup>Cu<sup>(2+)</sup> sample according to the EN ISO 10319:2015-08 standard [70].

Parameter		COT	COT-ALG <sup>(-)</sup> Na <sup>(+)</sup> (1%)	COT-ALG <sup>(-)</sup> Na <sup>(+)</sup> (9.7%)	COT-ALG <sup>(-)</sup> Cu <sup>(2+)</sup> (0.15)	COT-ALG <sup>(-)</sup> Cu <sup>(2+)</sup> (0.28)
Tensile strength (N)	(a)	490 ± 10	510 ± 30	580 ± 10	513 ± 25	515 ± 20
	(b)	380 ± 10	370 ± 70	410 ± 20	375 ± 50	380 ± 60
Relative elongation at maximum load (%)	(a)	7.6 ± 1.6	11.0 ± 1.5	10.0 ± 1.5	11.0 ± 1.6	11.0 ± 1.5
	(b)	28.0 ± 2.0	34.5 ± 3.5	29.5 ± 3.0	35.1 ± 4.0	33.4 ± 4.3

The results have been measured in duplicate and are presented as the mean value with ± deviation of approximately 2%; (a): parallel direction; (b): transverse direction.

The results show the increase in tensile strength after the alginate modification of the cotton material (COT-ALG<sup>(-)</sup>Na<sup>(+)</sup>(1%): 510/370 and COT-ALG<sup>(-)</sup>Na<sup>(+)</sup>(9.7%): 580/410 kN/m) in comparison with the unmodified sample (COT: 490/380 kN/m). The

higher the concentration of sodium alginate, the higher the tensile strength. The subsequent immersion in  $\text{CuCl}_2$  did not influence the tensile strength. Similarly, there was a slight increase in the relative elongation for the sample modified with 0.5% solution of sodium alginate; however, it decreased with the increase in the sodium alginate concentration (Table 6). Further modification with  $\text{CuCl}_2$  did not affect the relative elongation.

### 2.3. Biological and Biochemical Properties

#### 2.3.1. Antimicrobial Activity

The antimicrobial activity of COT-ALG<sup>(-)</sup>Cu<sup>(2+)</sup> composites and COT-Cu<sup>(2+)</sup> samples was investigated through the disk diffusion method using Gram-negative (*Escherichia coli*, *Pseudomonas aeruginosa*) and Gram-positive (*Staphylococcus aureus*) bacteria and the representative fungus species (*Chaetomium globosum*, *Candida albicans*). The results of the antibacterial and antifungal activity test according to the EN-ISO 20645:2006 [71] and the EN 14119:2005 [72] standards are presented in Tables 8 and 9, and the images are shown in Figures 6–8.

**Table 8.** Results of antimicrobial activity tests of alginate composites on the basis of the EN-ISO 20645:2006 standard [71].

Sample Name	Average Inhibition Zone (mm)		
	<i>E. coli</i>	<i>S. aureus</i>	<i>P. aeruginosa</i>
COT	0	0	0
COT-ALG <sup>(-)</sup> Na <sup>(+)</sup> (1%)	0	0	0
COT-ALG <sup>(-)</sup> Na <sup>(+)</sup> (9.7%)	0	0	0
COT-Cu <sup>(2+)</sup> (0.16)	2	2	2
COT-Cu <sup>(2+)</sup> (0.30)	3	4	4
COT-ALG <sup>(-)</sup> Cu <sup>(2+)</sup> (0.15)	3	2	2
COT-ALG <sup>(-)</sup> Cu <sup>(2+)</sup> (0.28)	5	4	3

Concentration of inoculum (CFU/mL): *E. Coli*— $2.1 \times 10^8$ , *S. Aureus*— $1.9 \times 10^8$ , *Ch. Globosum*— $2.0 \times 10^6$ , *P. aeruginosa*— $2.2 \times 10^8$ .

**Table 9.** Results of antimicrobial activity tests of alginate composites on the basis of the EN 14119:2005 standard [72].

Sample Name	Average Inhibition Zone (mm)	
	<i>Ch. globosum</i>	<i>C. albicans</i>
COT	0	0
COT-ALG <sup>(-)</sup> Na <sup>(+)</sup> (1%)	0	0
COT-ALG <sup>(-)</sup> Na <sup>(+)</sup> (9.7%)	0	0
COT-Cu <sup>(2+)</sup> (0.16)	no growth	no growth
COT-Cu <sup>(2+)</sup> (0.30)	no growth	no growth
COT-ALG <sup>(-)</sup> Cu <sup>(2+)</sup> (0.15)	no growth	no growth
COT-ALG <sup>(-)</sup> Cu <sup>(2+)</sup> (0.28)	no growth	no growth

Concentration of inoculum (CFU/mL): *Ch. Globosum*— $2.0 \times 10^6$ , *C. albicans*— $0.8 \times 10^8$ .

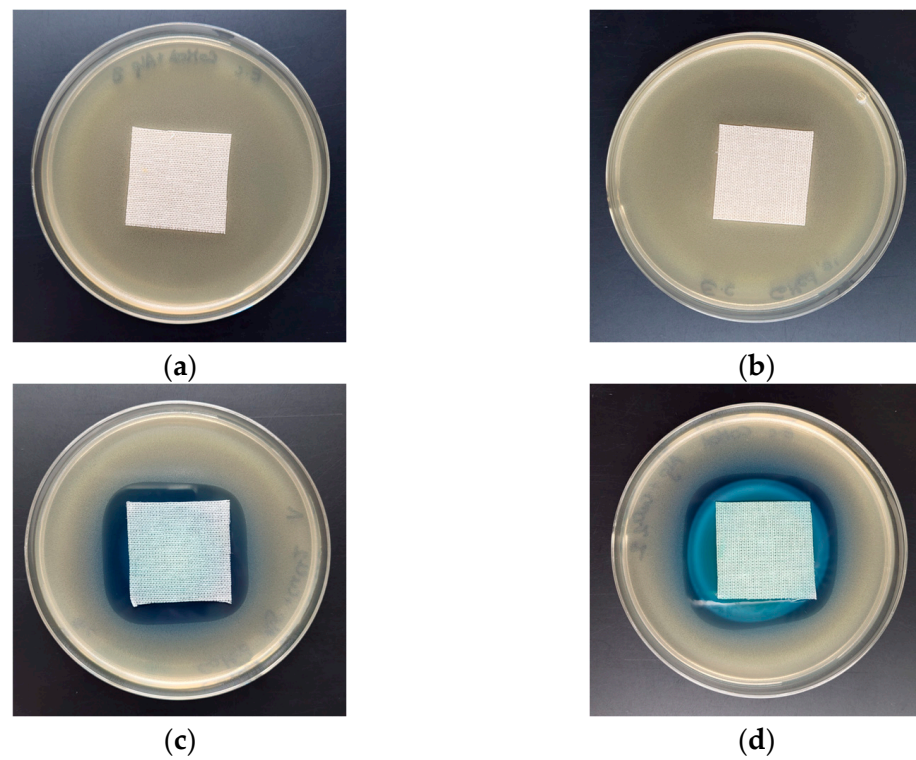


**Figure 6.** Tests of antimicrobial activity of alginate composites against *E. coli*; inhibition zones of bacterial growth in Petri dishes: (a) COT; (b) COT-ALG<sup>(-)</sup>Na<sup>(+)</sup>(1%); (c) COT-ALG<sup>(-)</sup>Cu<sup>(2+)</sup>(0.15); (d) COT-ALG<sup>(-)</sup>Cu<sup>(2+)</sup>(0.28).

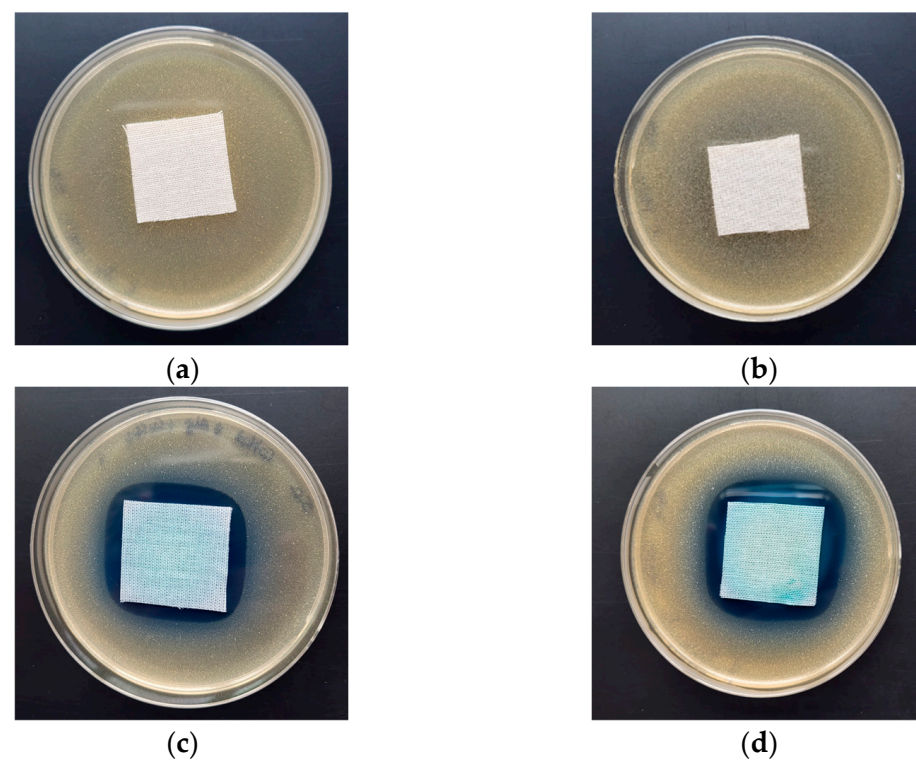


**Figure 7.** Tests of antimicrobial activity of alginate composites against *S. aureus*; inhibition zones of bacterial growth in Petri dishes: (a) COT; (b) COT-ALG<sup>(-)</sup>Na<sup>(+)</sup>(1%); (c) COT-ALG<sup>(-)</sup>Cu<sup>(2+)</sup>(0.15); (d) COT-ALG<sup>(-)</sup>Cu<sup>(2+)</sup>(0.28).

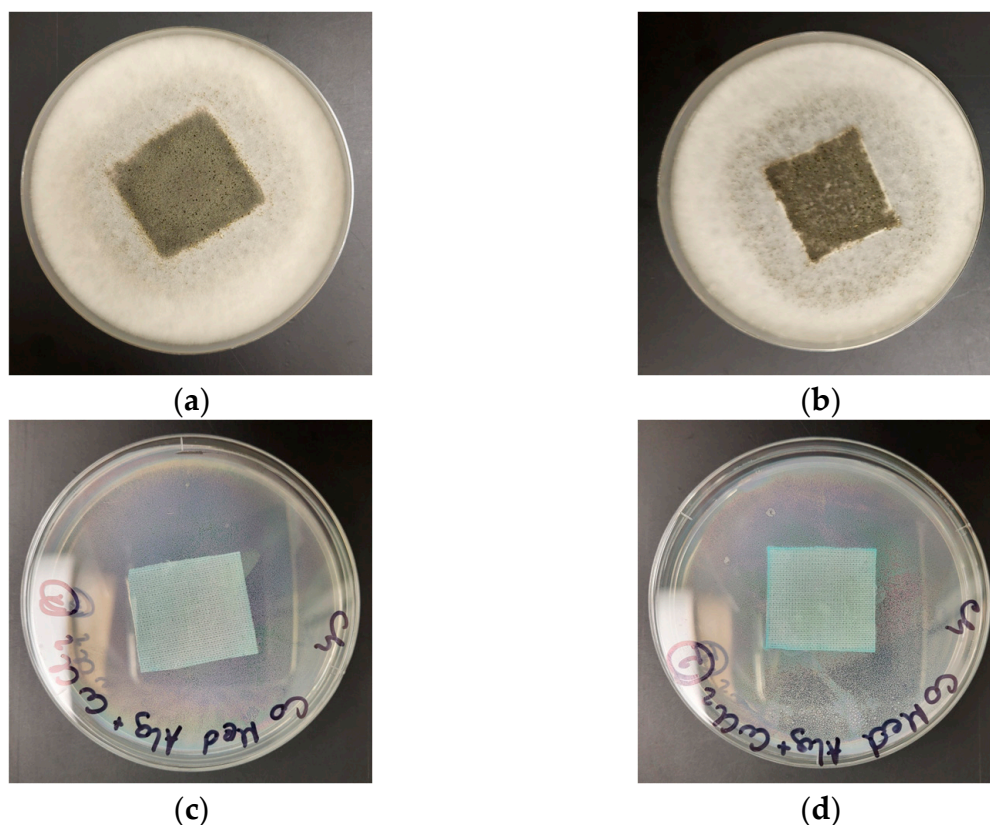


**Figure 8.** Tests of antimicrobial activity of alginate composites against *Ch. globosum*; inhibition zones of bacterial growth in Petri dishes: (a) COT; (b) COT-ALG<sup>(-)</sup>Na<sup>(+)</sup>(1%); (c) COT-ALG<sup>(-)</sup>Cu<sup>(2+)</sup>(0.15); (d) COT-ALG<sup>(-)</sup>Cu<sup>(2+)</sup>(0.28).

Control samples—the unmodified cotton material (COT) and the material modified with alginic acid sodium salt (COT-ALG<sup>(-)</sup>Na<sup>(+)</sup>) exhibited strong growth of bacterial and fungal colonies covering the entire surface of the samples placed on Petri dishes (Figures 6–8). Cotton material functionalized by copper (COT-Cu<sup>(2+)</sup>) and copper/alginate complex (COT-ALG<sup>(-)</sup>Cu<sup>(2+)</sup>) showed an inhibitory effect against *E. coli*, *S. aureus*, and *P. aeruginosa* bacteria and fungus species expressed by zones of inhibition, with no visible growth on/under the samples (Tables 8 and 9, Figures 6–9).

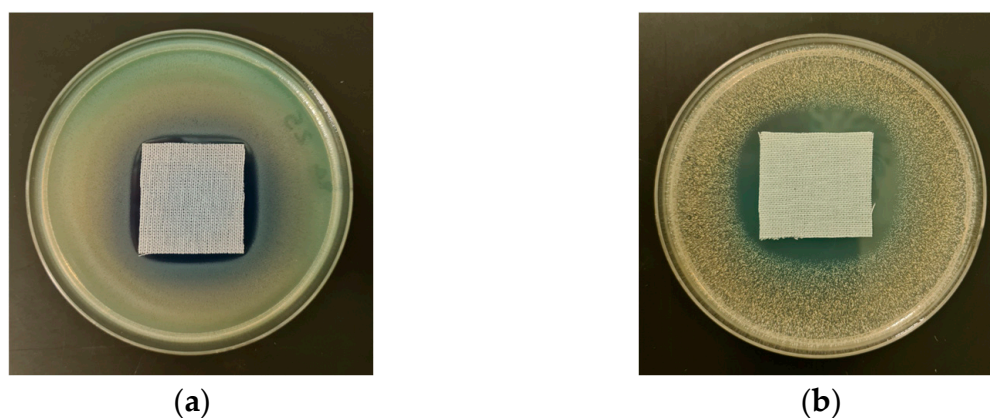


**Figure 9.** Tests of antimicrobial activity of COT-Cu<sup>(2+)</sup>(0.30) against *P. aeruginosa* (a) and *S. aureus* (b)—inhibition zones of bacterial growth in Petri dishes according to the EN-ISO 20645:2006 standard.

The obtained results show that the simultaneous modification with copper and alginate allows for a superior antibacterial effect against the *E. coli* bacteria. For samples modified

with the same solution of  $\text{CuCl}_2$ , i.e., 5% and 10%, the inhibition zones were higher in the case of cotton–alginate composites (3 mm and 5 mm, respectively) than for cotton samples (2 mm and 3 mm, respectively). At the same time, no significant difference in the antimicrobial activity was observed for other tested microorganisms.

The results obtained in accordance with the EN-ISO 20645:2006 and EN 14119:2005 standards [71,72] confirmed the antimicrobial protection of cotton–alginate–copper composite materials ( $\text{COT-ALG}^{(-)}\text{Cu}^{(2+)}$ ) against various type of microorganisms. This is in agreement with our previous work on the antimicrobial properties of alginate–copper complexes [40]. These results are comparable also with Grace et al.'s data [73].

### 2.3.2. Blood Plasma Clotting: aPTT and PT

The studied composites ( $\text{COT-ALG}^{(-)}\text{Na}^{(+)}$  and  $\text{COT-ALG}^{(-)}\text{Cu}^{(2+)}$ ) did not have a significant noxious effect on blood plasma coagulation (PT and aPTT), except  $\text{COT-ALG}^{(-)}\text{Cu}^{(2+)}(0.28)$  (Cu concentration: 17.51 g/kg), where only aPTT was extended. The materials without alginate ( $\text{COT-Cu}^{(2+)}$ ) had a much more prolonged aPTT with increasing copper concentration; however, no effect on PT was observed (Figures 10 and 11). Copper in the samples led to some inhibition of contact clotting activation in human blood plasma, as indicated by the prolongation of aPTT, but this effect disappeared in the presence of the alginate at the lower copper concentration, and even at the higher copper concentration, the inhibition was still lower than in the absence of the alginate. There was no effect on PT, regardless of the presence or absence of the alginate, so only contact factors (XI, XII, HK) were probably adsorbed on  $\text{Cu}^{2+}$  ions, which contributed to a decrease in their concentration in plasma and thus the effect of aPTT prolongation, but alginate abolished this effect. There was no increased activation of the coagulation cascade in the extrinsic pathway; therefore, the remaining elements of both pathways and coagulation cascades were not affected. This conclusion is also justified in light of the few studies on the influence of transition metals on contact proteins, including examining copper, nickel, cobalt, and zinc cations in the second oxidation state enclosed in liposomes, which showed the influence on aPTT and the absorption of factors XI, XII, and HK in human plasma [74,75]. Such properties of copper may therefore have an adverse effect on blood coagulation when used for the production of dressing materials, despite its beneficial antimicrobial properties. Regardless of this phenomenon, other material modifications with alginate and copper together (in relatively low concentrations of Cu ( $\text{COT-ALG}^{(-)}\text{Cu}^{(2+)}(0.15)$ )) had no negative influence on coagulation, so alginate might be used as a protective component of the composite, thus eliminating the harmful effect on the internal coagulation pathway. Such novel composite materials could potentially be used as neutral for blood clotting and antibacterial dressing materials, taking into account their favorable antibacterial copper-derived properties examined in this study and the alginate layer balancing the blood clotting.

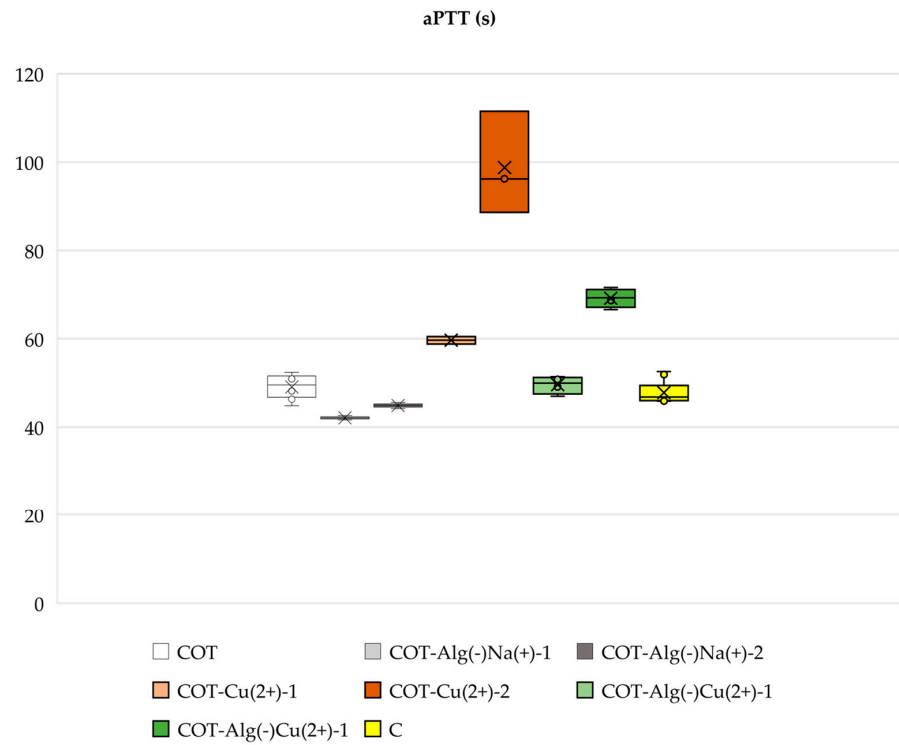


**Figure 10.** Effect of studied alginate composites on aPTT: COT; COT-ALG<sup>(-)</sup>Na<sup>(+)</sup>(1%); COT-ALG<sup>(-)</sup>Na<sup>(+)</sup>(9.7%); COT-Cu<sup>(2+)</sup>(0.16); COT-Cu<sup>(2+)</sup>(0.30); COT-ALG<sup>(-)</sup>Cu<sup>(2+)</sup>(0.15); COT-ALG<sup>(-)</sup>Cu<sup>(2+)</sup>(0.28); and C—control sample: plasma not exposed to composites. Results are presented as mean (×), median (horizontal line), range (bars), and interquartile range (box).

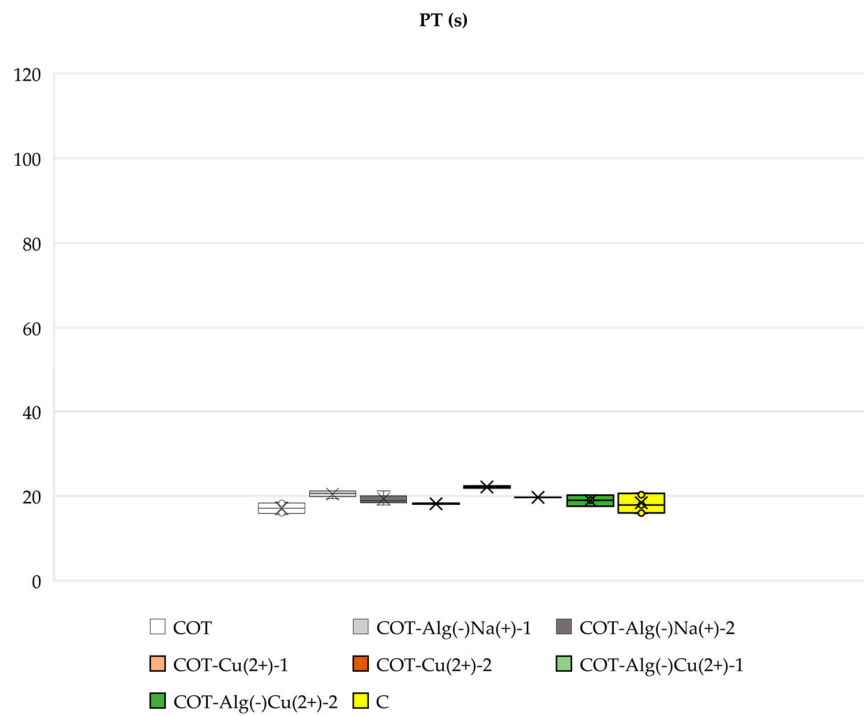


**Figure 11.** Effect of studied alginate composites on PT: COT; COT-ALG<sup>(-)</sup>Na<sup>(+)</sup>(1%); COT-ALG<sup>(-)</sup>Na<sup>(+)</sup>(9.7%); COT-Cu<sup>(2+)</sup>(0.16); COT-Cu<sup>(2+)</sup>(0.30); COT-ALG<sup>(-)</sup>Cu<sup>(2+)</sup>(0.15); COT-ALG<sup>(-)</sup>Cu<sup>(2+)</sup>(0.28); and C—control sample: plasma not exposed to composites. Results are presented as mean (×), median (horizontal line), range (bars), and interquartile range (box).

### 3. Conclusions

Antimicrobials neutral for blood clotting wound dressing composites could help to solve the contemporaneous challenges of antimicrobial regenerative medicine, especially those related to antibiotic resistance during wound dressing and care. In this study, we have developed and characterized composite materials consisting of: alginic acid sodium salt, cotton, and copper (II) with different selected concentrations of cations of the tested metal. The cotton–alginate–copper composites were prepared through a two-step, dip-coating procedure. The chemical and structural characterizations of the alginate composites were obtained through Fourier Transform Infrared Spectroscopy (FTIR), Flame Atomic Absorption Spectrometry (FAAS), Specific Surface Area (BET), determination of the air filtration parameters, and tensile strength measurements. The obtained materials exhibited antimicrobial in vitro activity against representative Gram-positive/negative bacteria and representative fungus species. The evaluation of the biochemical properties of the new composites was carried out in the area of blood plasma coagulation processes, including: activated partial thromboplastin time (aPTT), prothrombin time (PT), and thrombin time (TT). The biological results showed that complexes of Cu–alginate with antimicrobial properties at appropriately selected  $\text{Cu}^{2+}$  concentrations had no significant effect on blood plasma coagulation processes, but they still exhibited antimicrobial activity, in contrast to the material based only on cotton and copper, which showed unfavorable properties prolonging clotting in the intrinsic pathway demonstrated by the extension of aPTT. From this point of view, the obtained cotton–alginate–copper composites might be promising materials for biomedical applications, e.g., wound dressing. The great advantage of the cotton–alginate–copper materials in terms of implementation is the low cost and high availability of its components, and the uncomplicated production process. For future clinical applications, it is critical to test the antimicrobial cotton–alginate–copper composites not only against clinically isolated microbes, but also against multidrug-resistant strains, and to evaluate the in vitro and in vivo biocompatibility, as well as to assess blood coagulation and wound care by applying in vivo mammalian model systems [66]. Negligible moderate neutrality for blood clotting and antibacterial toxicity of the new composites might find great potential in the dressing and healing of wounds with simultaneous prevention and treatment of infections.

### 4. Materials and Methods

#### 4.1. Materials

- Alginic acid sodium salt (CAS Number 9005-38-3; molecular weight: 120,000–190,000 g/mol; mannuronic acid to guluronic acid–M/G ratio: 1.56) from Millipore Sigma (St. Louis, MO, USA) was used for the surface modification of polymer nonwovens;
- Medical fabric with a plain weave, qualitative composition: cotton (100% *w/w*), weight: 200 g/m<sup>2</sup> (Andropol S.A., Andrychów, Poland);
- Copper(II) chloride,  $\text{CuCl}_2$ , 97% (CAS Number: 7447-39-4) from Millipore Sigma (St. Louis, MO, USA) was used for surface modification of the nonwoven composite;
- Bacterial strains: *E. coli* (ATCC 25922), *S. aureus* (ATCC 6538), and *P. aeruginosa* (ATCC 27853) were purchased from Microbiologics (St. Cloud, MN, USA);
- Fungal strains: *C. albicans* (ATCC 10231) and *Ch. globosum* (ATCC 6205) were purchased from Microbiologics (St. Cloud, MN, USA).
- Standard human blood plasma lyophilizates and clotting times reagents (Dia-PTT, Dia-PT, 0.025 M  $\text{CaCl}_2$  solution) were obtained from a vendor (Diagon Kft, Budapest, Hungary) and prepared according to the manufacturer's instructions for measurements (K-3002 OPTIC coagulometers, KSELMED<sup>®</sup>, Grudziądz, Poland).

## 4.2. Methods

### 4.2.1. Chemical and Structural Characterization

#### Attenuated Total Reflection–Fourier-Transform Infrared Spectroscopy (ATR-FTIR)

The chemical structure of the samples was assessed using ATR-FTIR spectroscopy in the range of 400–4000  $\text{cm}^{-1}$  using a spectrometer (Jasco's 4200 (Tokyo, Japan)) with the ATR attachment Pike Gladi ATR (Cottonwood, AZ, USA).

#### Flame Atomic Absorption Spectroscopy (FAAS)

Determination of the copper content in alginate composites was assessed through the FAAS method in a similar way to that described earlier [35,37]. The sample was mineralized using a single-module Magnum II microwave mineralizer from Ertec (Wroclaw, Poland). The determination of the copper (II) ions was performed through atomic absorption spectrometry with flame excitation using a Thermo Scientific Thermo Solar M6 spectrometer (LabWrench, Midland, ON, Canada). The measurements were made in triplicate, and the results were presented as a mean value.

#### Microscopy Analysis

The morphology of the investigated samples was assessed using a VHX-7000N digital microscope (Keyence, Japan). The applied magnification was equal to  $\times 500$  and  $\times 2500$ . The microscope was equipped with the EA-300 laser-based elemental analyzer, which uses laser-induced breakdown spectroscopy (LIBS) to assess the elemental composition of the sample.

#### Specific Surface Area

The specific surface area was determined through the Brunauer, Emmet, and Teller method (BET). Measurements were carried out using the Autosorb-1 apparatus (Quantachrome Instruments, Boynton Beach, FL, USA), with nitrogen as a sorption agent and an adsorption isotherm at 77 K. In each experiment, approximately 1–2 g of a given sample was weighed and used. Prior to the analysis, the samples were dried in 105 °C for 24 h and degassed at room temperature. Measurements were made in duplicate, and the results were presented as a mean value.

#### Air Filtration Parameters

Air permeability of the cotton–alginate–copper composites was determined according to the EN ISO 9237:1998 standard [69]. The FX 3300 TEXTEST AG (Klimatest, Poland) permeability tester was used. Air at a pressure of 100 Pascal was passed through a fabric area of 20  $\text{cm}^2$  diameter for testing.

#### Tensile Testing

Tensile testing of the cotton–alginate–copper composites was carried out in accordance with the EN ISO 10319:2015-08 standard [70]. An Tinius Olsen H50KS (USA) tester was used. The stretching speed was 20 mm/min.

### 4.2.2. Antimicrobial Activity

The antibacterial activity of the COT-Alg<sup>(-)</sup>Cu<sup>(2+)</sup> material was assessed according to standard PN-EN ISO 20645:2006 against a representative colony of Gram-negative and Gram-positive bacteria (*E. coli*, *S. aureus*, and *P. aeruginosa*) [71]. The antifungal activity of the composites was tested according to PN-EN 14119:2005 against *Ch. globosum* (ATCC 6205) and *C. albicans* (ATCC 10231) [72]. All tests were carried out in duplicate.

### 4.2.3. Activated Partial Thromboplastin Time (aPTT) and Prothrombin Time (PT)

Pieces of the studied fabrics (1 mg square slices) were supplemented with 200  $\mu\text{L}$  plasma samples and vortexed and incubated for 15 min at 37 °C. Control samples that were not exposed to composites were also incubated for 15 min at 37 °C. The aPTT was

completed for each sample. First, 50  $\mu\text{L}$  of the plasma sample and 50  $\mu\text{L}$  of the suspension of Dia-PTT were added to a cuvette located in the thermostat of the coagulometer (37 °C) and left for 3 min. The measurements were initiated by inserting 50  $\mu\text{L}$  of 0.025 M  $\text{CaCl}_2$ . The PT was then run: plasma (50  $\mu\text{L}$ ) was kept warm (37 °C) in the thermostat of the coagulometer for 2 min, and Dia-PT (50  $\mu\text{L}$ ) was added to start the measurement.

**Author Contributions:** Z.M. developed the concept and designed the experiments, performed the experiments, analyzed the data, and wrote the paper; M.P. developed the concept, performed the blood coagulation experiments, and analyzed the data; A.K. performed the experiments, analyzed the data, and wrote the paper; M.B. designed the experiment for alginate modification; E.S. analyzed the data; M.H.K. developed the concept and designed the experiments, analyzed the data, and wrote the paper. All authors have read and agreed to the published version of the manuscript.

**Funding:** This research was partly carried out within the National Science Centre project number M-ERA.NET 2022, No. 2022/04/Y/ST4/00157.

**Institutional Review Board Statement:** Not applicable.

**Data Availability Statement:** The original data are available on request.

**Acknowledgments:** The authors would like to thank Dawid Chojnowski for technical contributions.

**Conflicts of Interest:** The authors declare no conflict of interest.

## References

1. Granados, A.; Pleixats, R.; Vallribera, A. Recent advances on antimicrobial and anti-inflammatory cotton fabrics containing nanostructures. *Molecules* **2021**, *26*, 3008. [[CrossRef](#)] [[PubMed](#)]
2. Shahriari-Khalaji, M.; Alassod, A.; Nozhat, Z. Cotton-based health care textile: A mini review. *Polym. Bull.* **2022**, *79*, 10409–10432. [[CrossRef](#)]
3. Venkatraja, B.; Malathy, V.V.; Elayarajah, B.; Rajendran, M.R.; Rammohan, R. Biopolymer and *Bletilla striata* herbal extract coated cotton gauze preparation for wound healing. *J. Med. Sci.* **2012**, *12*, 148–160. [[CrossRef](#)]
4. Emam, H.E. Antimicrobial cellulosic textiles based on organic compounds. *3 Biotech* **2019**, *9*, 29. [[CrossRef](#)] [[PubMed](#)]
5. Hegde, V.; Uthappa, U.T.; Altalhi, T.; Jung, H.Y.; Han, S.S.; Kurkuri, M.D. Alginate based polymeric systems for drug delivery, antibacterial/microbial, and wound dressing applications. *Mater. Today Commun.* **2022**, *33*, 104813. [[CrossRef](#)]
6. He, Q.; Tong, T.; Yu, C.; Wang, Q. Advances in algin and alginate-hybrid materials for drug delivery and tissue engineering. *Mar. Drugs* **2022**, *21*, 14. [[CrossRef](#)]
7. Sahoo, D.R.; Biswal, T. Alginate and its application to tissue engineering. *SN Appl. Sci.* **2021**, *1*, 30. [[CrossRef](#)]
8. Li, J.; He, J.; Huang, Y. Role of alginate in antibacterial finishing of textiles. *Int. J. Biol. Macromol.* **2017**, *94*, 466–473. [[CrossRef](#)] [[PubMed](#)]
9. Zhang, H.; Cheng, J.; Ao, Q. Preparation of alginate-based biomaterials and their applications in biomedicine. *Mar. Drugs* **2021**, *19*, 264. [[CrossRef](#)]
10. Zhang, M.; Zhao, X. Alginate Hydrogel Dressings for Advanced Wound Management. *Int. J. Biol. Macromol.* **2020**, *162*, 42. [[CrossRef](#)]
11. Garcia, T.D.F.; Silva, P.G.A.; Barcelos, B.J.; Miranda, M.D.G.R.D.; Alonso, C.D.S.; Abreu, M.N.S.; Borges, E.L. Criteria to Evaluate the Quality of Alginate Wound Dressings. *Rev. Bras. Enferm.* **2021**, *74*, e20201091. [[CrossRef](#)] [[PubMed](#)]
12. Barbu, A.; Neamtu, B.; Zăhan, M.; Iancu, G.M.; Bacila, C.; Mireșan, V. Current Trends in Advanced Alginate-Based Wound Dressings for Chronic Wounds. *J. Pers. Med.* **2021**, *11*, 890. [[CrossRef](#)] [[PubMed](#)]
13. Aderibigbe, B.A.; Buyana, B. Alginate in Wound Dressings. *Pharmaceutics* **2018**, *10*, 42. [[CrossRef](#)] [[PubMed](#)]
14. Soleimanpour, M.; Mirhaji, S.S.; Jafari, S.; Derakhshankhah, H.; Mamashli, F.; Nedaei, H.; Karimi, M.R.; Motasadizadeh, H.; Fatahi, Y.; Ghasemi, A.; et al. Designing a new alginate-fibrinogen biomaterial composite hydrogel for wound healing. *Sci. Rep.* **2022**, *12*, 7213. [[CrossRef](#)] [[PubMed](#)]
15. Xie, Y.; Gao, P.; He, F.; Zhang, C. Application of alginate-based hydrogels in hemostasis. *Gels* **2022**, *8*, 109. [[CrossRef](#)]
16. Hurtado, A.; Aljabali, A.A.; Mishra, V.; Tambuwala, M.M.; Serrano-Aroca, A. Alginate: Enhancement strategies for advanced applications. *Int. J. Mol. Sci.* **2022**, *23*, 4486. [[CrossRef](#)]
17. Varaprasad, K.; Jayaramudu, T.; Kanikireddy, V.; Toro, C.; Sadiku, E.R. Alginate-based composite materials for wound dressing application: A mini review. *Carbohydr. Polym.* **2020**, *236*, 116025. [[CrossRef](#)]
18. Raus, R.A.; Wan Nawawi, W.M.F.; Nasaruddin, R.R. Alginate and alginate composites for biomedical applications. *Asian J. Pharm. Sci.* **2021**, *16*, 280–306. [[CrossRef](#)]
19. Essa, E.A.; Elebyary, T.T.; Abdelquader, M.M.; El Maghraby, G.M.; Elkordy, A.A. Smart liquids for oral controlled drug release: An overview of alginate and non-alginate based systems. *J. Drug Deliv. Sci. Technol.* **2021**, *61*, 102211. [[CrossRef](#)]

20. Zdiri, K.; Cayla, A.; Elamri, A.; Erard, A.; Salaun, F. Alginate-based bio-composites and their potential applications. *J. Funct. Biomater.* **2022**, *13*, 117. [[CrossRef](#)] [[PubMed](#)]
21. Pino, P.; Bosco, F.; Mollea, C.; Onida, B. Antimicrobial Nano-Zinc Oxide biocomposites for wound healing applications: A Review. *Pharmaceutics* **2023**, *15*, 970. [[CrossRef](#)] [[PubMed](#)]
22. Rinaudo, M. Biomaterials based on a natural polysaccharide: Alginate. *TIP* **2014**, *17*, 92–96. [[CrossRef](#)]
23. Lv, C.; Zhou, X.; Wang, P.; Li, J.; Wu, Z.; Jiao, Z.; Guo, M.; Wang, Z.; Wang, Y.; Wang, L.; et al. Biodegradable alginate-based sponge with antibacterial and shape memory properties for penetrating wound hemostasis. *Compos. B Eng.* **2022**, *247*, 110263. [[CrossRef](#)]
24. Orłowska, J.; Kurczewska, U.; Derwinska, K.; Orłowski, W.; Orszulak-Michalak, D. In vitro evaluation of immunogenic properties of active dressings. *Curr. Issues Pharm. Med. Sci.* **2014**, *27*, 55–60. [[CrossRef](#)]
25. Cleetus, C.M.; Primo, F.A.; Fregoso, G.; Raveendran, N.L.; Noveron, J.C.; Spencer, C.T.; Ramana, C.V.; Joddar, B. Alginate hydrogels with embedded zno nanoparticles for wound healing therapy. *Int. J. Nanomed.* **2020**, *15*, 5097–5111. [[CrossRef](#)] [[PubMed](#)]
26. Segal, H.C.; Hunt, B.J.; Gilding, K. The effects of alginate and non-alginate wound dressings on blood coagulation and platelet activation. *J. Biomater. Appl.* **1998**, *12*, 249–257. [[CrossRef](#)] [[PubMed](#)]
27. Kamoun, E.A.; Kenawy, E.R.S.; Tamer, T.M.; El-Meligy, M.A.; Eldin, M.S.M. Poly (vinyl alcohol)-alginate physically crosslinked hydrogel membranes for wound dressing applications: Characterization and bio-evaluation. *Arab. J. Chem.* **2015**, *8*, 38–47. [[CrossRef](#)]
28. Rafiq, M.; Hussain, T.; Abid, S.; Nazir, A.; Masood, R. Development of sodium alginate/PVA antibacterial nanofibers by the incorporation of essential oils. *Mater. Res. Express* **2018**, *5*, 035007. [[CrossRef](#)]
29. Emam, H.E.; Manian, A.P.; Široká, B.; Duelli, H.; Merschak, P.; Redl, B.; Bechtold, T. Copper(I)oxide surface modified cellulose fibers—Synthesis, characterization and antimicrobial properties. *Surf. Coat. Technol.* **2014**, *254*, 344–351. [[CrossRef](#)]
30. Cady, N.C.; Behnke, J.L.; Strickland, A.D. Copper-based nanostructured coatings on natural cellulose: Nanocomposites exhibiting rapid and efficient inhibition of a multi-drug resistant wound pathogen, *A. baumannii*, and mammalian cell biocompatibility in vitro. *Adv. Funct. Mater.* **2011**, *21*, 2506–2514. [[CrossRef](#)]
31. Vincent, M.; Hartemann, P.; Engels-Deutsch, M. Antimicrobial applications of copper. *Int. J. Hyg. Environ. Health* **2016**, *219*, 585–591. [[CrossRef](#)]
32. Ingle, A.P.; Duran, N.; Rai, M. Bioactivity, mechanism of action, and cytotoxicity of copper-based nanoparticles: A review. *Appl. Microbiol. Biotechnol.* **2014**, *98*, 1001–1009. [[CrossRef](#)]
33. Kudzin, M.H.; Kaczmarek, A.; Mrozińska, Z.; Olczyk, J. Deposition of copper on polyester knitwear fibers by a magnetron sputtering system. physical properties and evaluation of antimicrobial response of new multi-functional composite materials. *Appl. Sci.* **2020**, *10*, 6990. [[CrossRef](#)]
34. Kudzin, M.H.; Boguń, M.; Mrozińska, Z.; Kaczmarek, A. Physical properties, chemical analysis, and evaluation of antimicrobial response of new Polylactide/Alginate/Copper Composite Materials. *Mar. Drugs* **2020**, *18*, 660. [[CrossRef](#)] [[PubMed](#)]
35. Kudzin, M.H.; Mrozińska, Z.; Kaczmarek, A.; Lisiak-Kucińska, A. Deposition of copper on poly(lactide) non-woven fabrics by magnetron sputtering—Fabrication of new multi-functional, antimicrobial composite materials. *Materials* **2020**, *13*, 3971. [[CrossRef](#)]
36. Borkow, G.; Gabbay, J. Putting copper into action: Copper-impregnated products with potent biocidal activities. *FASEB J.* **2004**, *18*, 1728–1730. [[CrossRef](#)] [[PubMed](#)]
37. Heliopoulos, N.S.; Papageorgiou, S.K.; Galeou, A.; Favvas, E.P.; Katsaros, F.K.; Stamatakis, K. Effect of copper and copper alginate treatment on wool fabric. Study of textile and antibacterial properties. *Surf. Coat. Technol.* **2013**, *235*, 24–31. [[CrossRef](#)]
38. Perelshstein, I.; Applerot, G.; Perkash, N.; Wehrschutz-Sigl, E.; Hasmann, A.; Guebitz, G.; Gedanken, A. CuO–cotton nanocomposite: Formation, morphology, and antibacterial activity. *Surf. Coat. Technol.* **2009**, *204*, 54–57. [[CrossRef](#)]
39. Emam, H.E.; Ahmed, H.B.; Bechtold, T. In-situ deposition of Cu<sub>2</sub>O micro-needles for biologically active textiles and their release properties. *Carbohydr. Polym.* **2017**, *165*, 255–265. [[CrossRef](#)]
40. Bajpai, S.K.; Bajpai, M.; Sharma, L. Copper nanoparticles loaded alginate-impregnated cotton fabric with antibacterial prop-erties. *J. Appl. Polym. Sci.* **2012**, *126*, E319–E326. [[CrossRef](#)]
41. Liu, J.; Zhang, R.; Ci, M.; Sui, S.; Zhu, P. Sodium alginate/cellulose nanocrystal fibers with enhanced mechanical strength prepared by wet spinning. *J. Eng. Fibers Fabr.* **2019**, *14*, 155892501984755. [[CrossRef](#)]
42. Bakil, S.N.A.; Kamal, H.; Abdullah, H.Z.; Idris, M.I. Sodium alginate-zinc oxide nanocomposite film for antibacterial wound healing applications. *Biointerface Res. Appl. Chem.* **2020**, *10*, 6245–6252. [[CrossRef](#)]
43. Klinkajon, W.; Supaphol, P. Novel copper (II) alginate hydrogels and their potential for use as anti-bacterial wound dressings. *Biomed. Mater.* **2014**, *9*, 045008. [[CrossRef](#)] [[PubMed](#)]
44. Mikołajczyk, T.; Wołowska-Czapnik, D. Multifunctional alginate fibres with anti-bacterial properties. *Fibres Text. East. Eur.* **2005**, *13*, 35–40. Available online: <https://www.semanticscholar.org/paper/Multifunctional-Alginate-Fibres-with-Anti-bacterial-Miko%25C5%2582ajczyk-Wo%25C5%2582owska-Czapnik/ed7706448cb20d28995d259f6aa47b79bf3a0825> (accessed on 31 August 2023).

45. Zare-Gachi, M.; Daemi, H.; Mohammadi, J.; Baei, P.; Bazgir, F.; Hosseini-Salekdeh, S.; Baharvand, H. Improving anti-hemolytic, antibacterial and wound healing properties of alginate fibrous wound dressings by exchanging counter-cation for infected full-thickness skin wounds. *Mater. Sci. Eng. C Mater. Biol. Appl.* **2020**, *107*, 110321. [[CrossRef](#)] [[PubMed](#)]
46. Wu, Y.; Han, G.T.; Gong, Y.; Zhang, Y.M.; Xia, Y.Z.; Yue, C.Q.; Wu, D.W. Antibacterial property and mechanism of copper alginate fiber. *Adv. Mater. Res.* **2010**, *152–153*, 1351–1355. [[CrossRef](#)]
47. Kim, J.O.; Choi, J.Y.; Park, J.K.; Kim, J.H.; Jin, S.G.; Chang, S.W.; Li, D.X.; Hwang, M.R.; Woo, J.S.; Kim, J.A.; et al. Development of clindamycin-loaded wound dressing with polyvinyl alcohol and sodium alginate. *Biol. Pharm. Bull.* **2008**, *31*, 2277–2282. [[CrossRef](#)] [[PubMed](#)]
48. Kornblatt, A.P.; Nicoletti, V.G.; Travaglia, A. The neglected role of copper ions in wound healing. *J. Inorg. Biochem.* **2016**, *161*, 1–8. [[CrossRef](#)] [[PubMed](#)]
49. Borkow, G.; Gabbay, J.; Dardik, R.; Eidelman, A.I.; Lavie, Y.; Grunfeld, Y.; Ikher, S.; Huszar, M.; Zatcoff, R.C.; Marikovsky, M. Molecular mechanisms of enhanced wound healing by copper oxide-impregnated dressings. *Wound Repair. Regen.* **2010**, *18*, 266–275. [[CrossRef](#)]
50. Cucci, L.M.; Satriano, C.; Marzo, T.; La Mendola, D. Angiogenin and copper crossing in wound healing. *Int. J. Mol. Sci.* **2021**, *22*, 10704. [[CrossRef](#)]
51. Tiwari, M.; Narayanan, K.; Thakar, M.B.; Jagani, H.V.; Rao, J.V. Biosynthesis and wound healing activity of copper nanoparticles. *IET Nanobiotechnol.* **2014**, *8*, 230–237. [[CrossRef](#)]
52. Cangul, I.T.; Gul, N.Y.; Topal, A.; Yilmaz, R. Evaluation of the effects of topical tripeptide-copper complex and zinc oxide on open-wound healing in rabbits. *Vet. Dermatol.* **2006**, *17*, 417–423. [[CrossRef](#)] [[PubMed](#)]
53. Alizadeh, S.; Seyedalipour, B.; Shafieyan, S.; Kheime, A.; Mohammadi, P.; Aghdami, N. Copper nanoparticles promote rapid wound healing in acute full thickness defect via acceleration of skin cell migration, proliferation, and neovascularization. *Biochem. Biophys. Res. Commun.* **2019**, *517*, 684–690. [[CrossRef](#)] [[PubMed](#)]
54. Sen, C.K.; Khanna, S.; Venojarvi, M.; Trikha, P.; Ellison, E.C.; Hunt, T.K.; Roy, S. Copper-induced vascular endothelial growth factor expression and wound healing. *Am. J. Physiol. Heart Circ. Physiol.* **2002**, *282*, H1821–H1827. [[CrossRef](#)]
55. Winter, W.E.; Flax, S.D.; Harris, N.S. Coagulation Testing in the Core Laboratory. *Lab. Med.* **2017**, *48*, 295–313. [[CrossRef](#)] [[PubMed](#)]
56. Kudzin, M.H.; Giełdowska, M.; Mrozińska, Z.; Boguń, M. Poly(lactic acid)/Zinc/Alginate complex material: Preparation and antimicrobial properties. *Antibiotics* **2021**, *10*, 1327. [[CrossRef](#)] [[PubMed](#)]
57. Kaputskii, V.E.; Komar, V.P.; Skorniyakov, I.V. Infrared spectra and structure of cellulose phosphates. *J. Appl. Spectrosc.* **1988**, *48*, 176–179. [[CrossRef](#)]
58. Lawrie, G.; Keen, I.; Drew, B.; Chandler-Temple, A.; Rintoul, L.; Fredericks, P.; Grøndahl, L. Interactions between alginate and chitosan biopolymers characterized using FTIR and XPS. *Biomacromolecules* **2007**, *8*, 2533–2541. [[CrossRef](#)]
59. Leal, D.; Matsuhira, B.; Rossi, M.; Caruso, F. FT-IR spectra of alginate acid block fractions in three species of brown seaweeds. *Carbohydr. Res.* **2008**, *343*, 308–316. [[CrossRef](#)] [[PubMed](#)]
60. Lim, S.F.; Zheng, Y.M.; Zou, S.W.; Chen, J.P. Characterization of copper adsorption onto an alginate encapsulated magnetic sorbent by a combined FT-IR, XPS, and mathematical modeling study. *Environ. Sci. Technol.* **2008**, *42*, 2551–2556. [[CrossRef](#)]
61. Cardenas-Jiron, G.; Leal, D.; Matsuhira, B.; Osorio-Roman, I.O. Vibrational spectroscopy and density functional theory calculations of poly-D-mannuronate and heteropolymeric fractions from sodium alginate: Vibrational spectroscopy of poly-D-mannuronate and heteropolymeric fractions from sodium alginate. *J. Raman Spectrosc.* **2011**, *42*, 870–878. [[CrossRef](#)]
62. Diaz-Visurraga, J.; Daza, C.; Pozo, C.; Becerra, A.; Von Plessing, C.; García, A. Study on antibacterial alginate-stabilized copper nanoparticles by FT-IR and 2D-IR correlation spectroscopy. *Int. J. Nanomed.* **2012**, *7*, 3597–3612. [[CrossRef](#)] [[PubMed](#)]
63. Nastaj, J.A.; Przewłocka, A.; Rajkowska-Myśliwiec, M. Biosorption of Ni(II), Pb(II) and Zn(II) on calcium alginate beads: Equilibrium, kinetic and mechanism studies. *Pol. J. Chem. Technol.* **2016**, *18*, 81–87. [[CrossRef](#)]
64. Fertah, M.; Belfkira, A.; Dahmane, E.M.; Taourirte, M.; Brouillette, F. Extraction and characterization of sodium alginate from Moroccan *Laminaria digitata* brown seaweed. *Arab. J. Chem.* **2017**, *10*, S3707–S3714. [[CrossRef](#)]
65. Airaksinen, S. *Role of Excipients in Moisture Sorption and Physical Stability of Solid Pharmaceutical Formulations*; University of Helsinki: Helsinki, Finland, 2005; ISBN 952-10-2733-9 (print), ISBN 952-10-2734-7 (pdf). ISSN 1795-7079.
66. Grada, A.; Mervis, J.; Falanga, V. Research techniques made simple: Animal models of wound healing. *J. Investig. Dermatol.* **2018**, *138*, 2095–2105. [[CrossRef](#)] [[PubMed](#)]
67. Thommes, M.; Kaneko, K.; Neimark, A.V.; Olivier, J.P.; Rodriguez-Reinoso, F.; Rouquerol, J.; Sing, K.S.W. Physisorption of gases, with special reference to the evaluation of surface area and pore size distribution (IUPAC Technical Report). *Pure Appl. Chem.* **2015**, *87*, 1051–1069. [[CrossRef](#)]
68. Qi, L.; Tang, X.; Wang, Z.; Peng, X. Pore characterization of different types of coal from coal and gas outburst disaster sites using low temperature nitrogen adsorption approach. *Int. J. Min. Sci. Technol.* **2017**, *27*, 371–377. [[CrossRef](#)]
69. EN ISO 9237:1998; Textiles—Determination of the Permeability of Fabrics to Air. International Organization for Standardization: Geneva, Switzerland, 1998.
70. EN ISO 10319:2015; Geosynthetics—Wide-Width Tensile Test. International Organization for Standardization: Geneva, Switzerland, 2015.

71. EN ISO 20645:2006; Textile Fabrics—Determination of Antibacterial Activity—Agar Diffusion Plate Test. International Organization for Standardization: Geneva, Switzerland, 2006.
72. PN-EN 14119: 2005 Point 10.5 (B2); Testing of Textiles—Evaluation of the Action of Microfungi—Visual Method. British Standards Institution: London, UK, 2005.
73. Grace, M.; Chand, N.; Bajpai, S.K. Copper alginate-cotton cellulose (CACC) fibers with excellent antibacterial properties. *J. Eng. Fibers Fabr.* **2009**, *4*, 24–35. [[CrossRef](#)]
74. Mutch, N.J.; Waters, E.K.; Morrissey, J.H. Immobilized transition metals stimulate contact activation and drive factor XII-mediated coagulation. *J. Thromb. Haemost.* **2012**, *10*, 2108–2115. [[CrossRef](#)]
75. Janisse, S.E.; Sharma, V.A.; Caceres, A.; Medici, V.; Heffern, M.C. Systematic evaluation of Copper(II)-loaded immobilized metal affinity chromatography for selective enrichment of copper-binding species in human serum and plasma. *Metallomics* **2022**, *14*, mfac059. [[CrossRef](#)]

**Disclaimer/Publisher’s Note:** The statements, opinions and data contained in all publications are solely those of the individual author(s) and contributor(s) and not of MDPI and/or the editor(s). MDPI and/or the editor(s) disclaim responsibility for any injury to people or property resulting from any ideas, methods, instructions or products referred to in the content.